Journal of South American Earth Sciences 32 (2011) 416–428

Contents lists available at ScienceDirect

Journal of South American Earth Sciences

journal homepage: www.elsevier.com/locate/jsames

U-Pb LA-MC-ICPMS geochronology of Cambro-Ordovician post-collisional granites of the Ribeira belt, southeast Brazil: Terminal Brasiliano magmatism in central Gondwana supercontinent

Claudio de Morisson Valeriano [a,*], Miguel Tupinambá [a], Antonio Simonetti [b], Monica Heilbron [a], Julio Cesar Horta de Almeida [a], Luiz Guilherme do Eirado [a]

[a] TEKTOS—Geotectonics Study Group, Universidade do Estado do Rio de Janeiro, Faculdade de Geologia, Rua São Francisco Xavier 524/4006-A, Rio de Janeiro, RJ 20559-900, Brazil
[b] Department of Civil Engineering and Geological Sciences, 156 Fitzpatrick Hall, University of Notre Dame, Notre Dame, IN 46556, USA

ARTICLE INFO

Article history:
Received 31 August 2010
Accepted 3 March 2011

Keywords:
Orogenic collapse
Slab break up
Anorogenic granite
Continental crust

ABSTRACT

New U-Pb ages for zircon and titanite obtained by LA-MC-ICPMS are reported for post-collisional granites from the central Ribeira belt (Rio de Janeiro State, southeast Brazil). These post-collisional, I-type, megaporphyritic and equigranular leucogranite plutons and dykes intrude high-grade metasedimentary units, orthogneisses, and migmatites within the root zone of the deeply eroded Neoproterozoic-Cambrian Ribeira belt. The ages obtained are: 511.2 ± 6.9 Ma (zircon) for the Suruí Granite; 490.3 ± 8.7 Ma (zircon) for a cross-cutting dyke of the pegmatitic facies of the Andorinha Granite from the same outcrop; 480.7 ± 6.1 Ma (zircon) for the Frades Granite; 488.7 ± 4.2 Ma (titanite) for the Nova Friburgo Granite; and 490.9 ± 9.8 Ma (zircon) for the Sana Granite. These new U-Pb ages and those compiled from the literature for post-orogenic intrusions distributed ~400 km along the strike of the orogen (Rio de Janeiro and Espírito Santo States), define two separate intervals for magmatic activity, which are consistent with mineralogical and structural signatures. The magmatic intervals consist of an older Cambrian magmatic pulse occurred at *ca.*512 Ma (Pedra Branca, Suruí and Buarama plutons), and a younger Ordovician event at *ca.* 486 Ma (Mangaratiba, Favela, Andorinha, Frades, Nova Friburgo and Sana granites). The Cambrian pulse post-dates the end of the first and main collisional phase by *ca.* 35 m.y. It also post-dates the onset of the second collisional episode by *ca.* 20 m.y. The late-Ordovician magmatic pulse post-dates the end of the second collisional episode by *ca.* 25 m.y. In map view, the alignment of the post-collisional plutons and stocks depicts a sinuous belt running along the eroded roots of central/northern Ribeira and Araçuaí belts. This granite belt probably marks the zone where preferential heating and melting of lower continental crust took place, either caused by breaking off of subducted slab, or by the extensional collapse of hot, overthickened continental crust.

1. Introduction and objectives

One of the most intriguing and less understood aspects of the tectonic evolution of collisional orogenic belts is their post-collisional stage, prior to the "stable" platform conditions that allow the development of intracratonic sag sedimentary basins. During the post-collisional stage of orogenesis crustal extension, uplift, decompression and melting concur in isostatic adjustment to anomalously hot and overthickened continental crust. This process is typically referred to as orogenic collapse (Rey et al., 2001). Development of extensional faulting in the upper crust typically results in the uplift of "hot" lower crust and leads to decompression melting (Ledru et al., 2001). This then generates pervasive anatexis and the voluminous migmatites and leucogranitic plutons (Vanderhaeghe and Teyssier, 2001). Post-collisional leucogranite emplacement in the upper crust is commonly associated with extensional faulting and sedimentary basin formation. Crustal extension commonly leads to the exhumation of lower crust granulite and/or migmatite core complexes.

For example, the well-exposed, post-collisional leucogranites from the central segment of the Ribeira belt (Rio de Janeiro State, southeast Brazil) intrude high-grade metasedimentary units, orthogneisses, and migmatites within the root of the deeply eroded internal zone of the Neoproterozoic-Cambrian orogenic belt. Their mode of occurrence varies from tabular bodies of centimeter to meter thickness, up to circular or elliptical plutons with diameters

* Corresponding author. Tel./fax: +55 21 2334 0533.
E-mail address: cmval@uerj.br (C.deM. Valeriano).

0895-9811/$ – see front matter © 2011 Elsevier Ltd. All rights reserved.
doi:10.1016/j.jsames.2011.03.003

varying from hundreds of meters up to ~20 km, in the case of the Sana Granite (Fig. 2).

This study presents new U-Pb ages of zircon and titanite for these post-collisional granitic plutons of Suruí, Andorinha, Frades, Três Picos, Nova Friburgo and Sana obtained by laser ablation-multicollector-inductively coupled plasma mass spectrometry (LA-MC-ICPMS). The new U-Pb data provide crystallization ages and temporal constraints, which in turn help to refine the timing of the different stabilization stages of the Ribeira orogenic belt. The results are also discussed in the context of the final stages of Gondwana formation during the Cambro-Ordovician.

2. Geologic context

2.1. The Ribeira belt in the Mantiqueira Province

The Mantiqueira Province (Fig. 1) is a 3000 km-long orogen that extends in roughly a NE-SW direction along the Atlantic coast of southeast-Brazil and Uruguay. Along with the Borborema and the Tocantins provinces, the Mantiqueira Province resulted from the "Brasiliano" (-Pan African) convergence and eventual collision of paleocontinental ("cratonic") blocks during the Neoproterozoic to Cambrian times, leading to the amalgamation of the West-Gondwana supercontinent.

The Araçuaí and Ribeira belts make up the northern part of the Mantiqueira Province which, in pre-Atlantic paleogeography, had the West Congo and Kaoko orogenic belts as their African counterparts (Pedrosa Soares et al., 2001). These belts formed a larger orogen between the São Francisco-Congo, Paranapanema and Kalahari paleocontinental blocks (Unrug, 1996).

2.2. The central Ribeira belt: the roots of an accretionary/collisional orogenic belt

One of the main characteristics of the Ribeira belt is the profusion of several generations of granites (Pires et al., 1982; Junho et al., 1987) that can be related to the pre-, syn- and post-collisional phases of the orogen. The central segment of the Ribeira belt (Fig. 2) is located to the south of the southern tip of the São Francisco craton, and is characterized by a long and complex history of terrane accretions against the former margin of this paleocontinent. From the cratonic area towards the internal zone of the

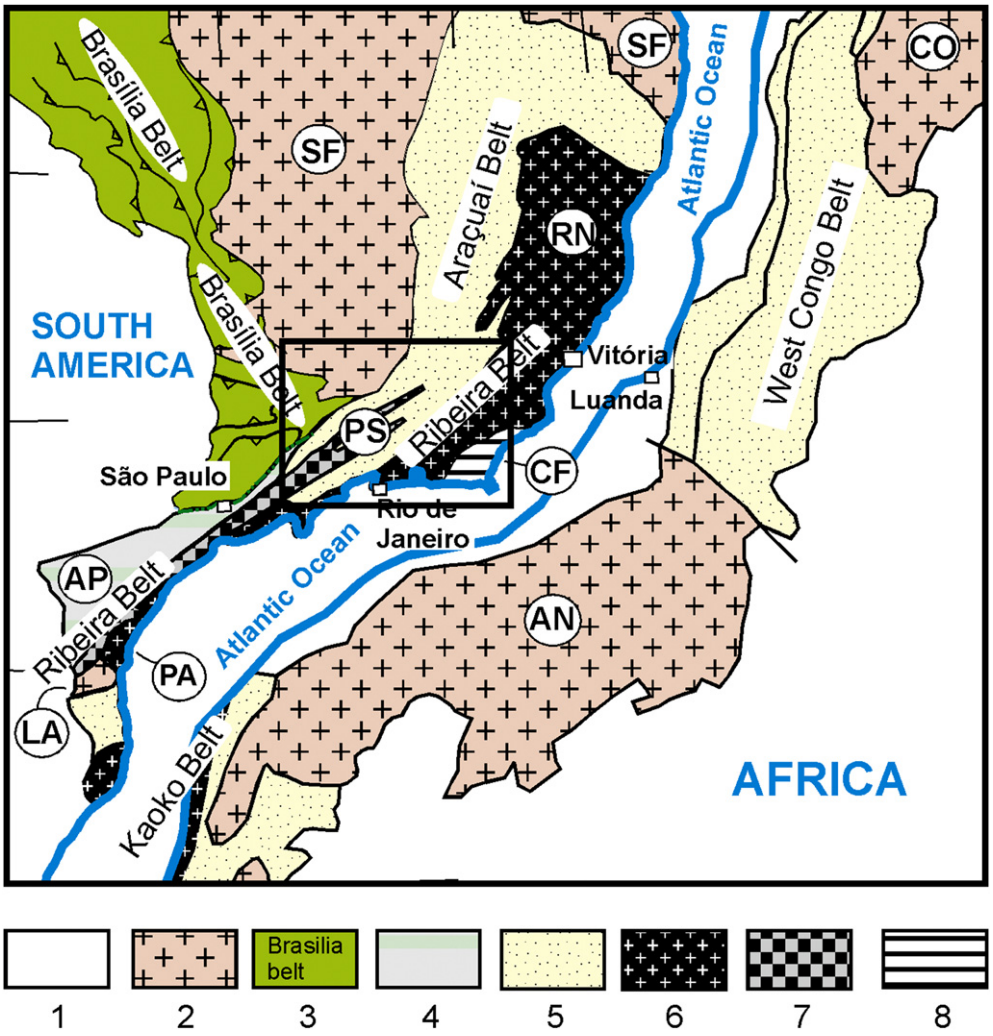

Fig. 1. The central segment of the Ribeira belt (rectangle), in the pre-Atlantic (Cretaceous) paleogeographic reconstruction of the Gondwana supercontinent (modified from Heilbron et al., 2008). The Brasiliano-Pan African orogenic realm comprises the Araçuaí/Ribeira/Dom Feliciano belts (Mantiqueira Province) and the West Congo/Kaoko belts, respectively in South America and Africa. Legend: 1- Phanerozoic cover; 2- Archean-Paleoproterozoic cratonic areas (SF- São Francisco, LA- Luis Alves, CO- Congo, AN- Angola); 3- Brasilia thrust-fold belt; 4- Apiaí terrane; 5- Brasiliano metasedimentary fold belt, 6- Accreted Neoproterozoic magmatic arcs (RN- Rio Negro, PA- Paranaguá); 7 –Paraíba do Sul terrane; 8 –Cabo Frio terrane.

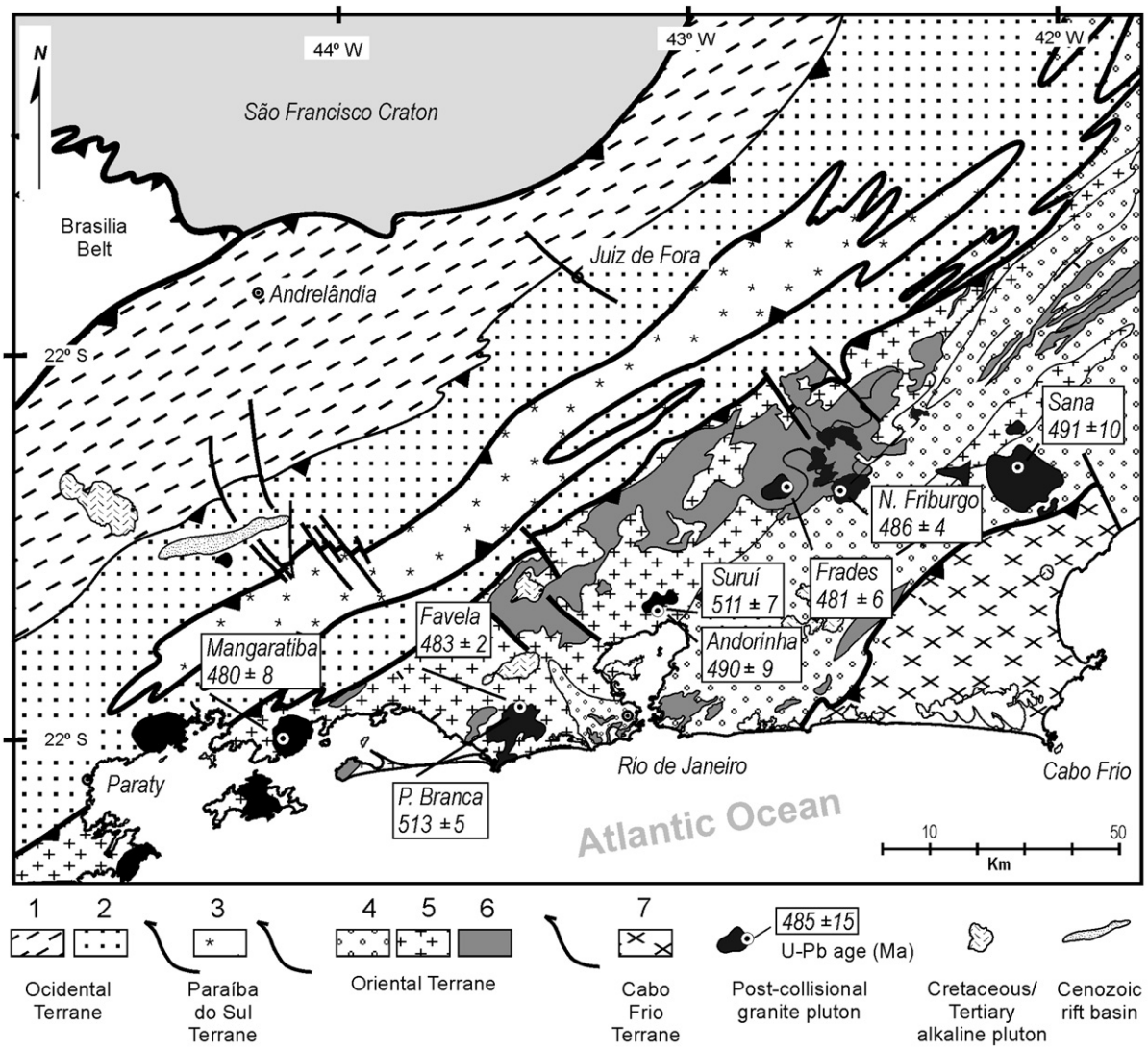

Fig. 2. Tectonic sketch map of the central segment of Ribeira Belt (modified from Heilbron and Machado, 2003). Legend: Occidental terrane (1 – Andrelândia domain; 2 – Juiz de Fora domain); 3 – Paraíba do Sul terrane; Oriental terrane (4 – Metasedimentary units; 5 – Rio Negro magmatic arc; 6 – Sin-collisional granitoid rocks); 7 – Cabo Frio terrane. The post-collisional intrusive complexes are represented in black, with respective U-Pb ages.

belt, where the granites examined in this study are located, metamorphic grade increases from greenschist to upper amphibolite and granulite facies. Following a protracted phase of pre-collisional magmatism (790–605 Ma) that formed the Rio Negro magmatic arc (Tupinambá et al., 2000; Heilbron and Machado, 2003; Heilbron et al., 2008), two main collisional episodes are recorded in the area, one at *ca*. 580-550 Ma and a later one at *ca*. 535-520 Ma. The latter collisional event is followed by the Cambrian-Ordovician post-collisional phase of the orogen, characterized by the emplacement of undeformed granites, aplites, and pegmatites associated to extensional structures, which are the focus of this work.

2.3. *ca.* 580-550 Ma collision

The first and main collisional episode took place between 580 Ma and 550 Ma, and was associated with granite generation and regional high-grade M1 metamorphism. This episode resulted from the collision between the Oriental Terrane, represented by the Rio Negro magmatic arc and the country rock paragneisses of the São Fidélis Complex, and the passive margin of the southern São Francisco Paleocontinent (the Occidental Terrane). The latter is represented by the Neoproterozoic metasedimentary rocks of the Andrelândia group. This collisional episode led to the development of several thrust systems affecting both the para-autochtonous and allochthonous metasedimentary rocks of the Andrelândia Group, and the granite-gneiss-greenstone rocks of the Paleoproterozoic-Archean basement associations. This episode resulted in the development of subhorizontal tight folding and associated main penetrative D1 and D2 foliations.

During this first collisional event, the high metamorphic grade para- and orthogneisses of the Oriental terrane were infiltrated by voluminous syn-collisional granitic veins, dykes, plutons and batholiths. The latter are typically represented by kilometer scale sills of calc-alkaline I-type K-feldspar megaporphyritic granite or augen gneiss (Mendes et al., 2006), (hornblende) biotite granite and S-type garnet leucogranite.

In Rio de Janeiro and adjoining Niterói cities, the Pão de Açúcar augen gneiss dominates the landscape, forming pinnacles and outstanding monoliths such as the “Sugar Loaf”. The latter is characterized by its lens-shaped texture of sheared K-feldspar megacrysts. Heilbron and Machado (2003) and Silva et al. (2003) conducted U-Pb dating of zircon from the augen gneiss at the

Sugar Loaf and Corcovado mountains by isotope dilution-thermal ionization mass spectrometry (ID-TIMS) and SHRIMP respectively, reporting crystallization ages of 578+/-19 Ma and *ca*. 560 Ma.

The Serra dos Órgãos batholith, which also represents the product of syn-collisional magmatism, outcrops as a thick sheet-like pluton intruding the older (Neoproterozoic) pre-collisional magmatic arc orthogneisses of the Rio Negro Complex. Fracture-controlled erosion of the latter two units result in sheer walls and pinnacles of the mountain ranges north of Rio de Janeiro, frequently forming summits of more than 2000 m above sea level. The Serra dos Órgãos batholith comprises coarse-grained, equigranular biotite (and/or hornblende) gneisses of granodioritic to granitic compositions that display either isotropic and flow foliation textures. U-Pb SHRIMP dating yielded a crystallization age of 569 +- 6 Ma (Silva et al., 2003). In addition to these two batholiths and other smaller plutonic lens-shaped bodies, numerous garnet-bearing, foliated leucogranitic bodies of varying sizes pervasively intrude the Rio Negro orthogneisses and the São Fidélis Group paragneisses, often showing transitions to diatexitic migmatites.

2.4. The ca. 535-520 Ma collision

The overprints resulting from deformation, metamorphism and granite generation at *ca*. 530-520 Ma are well characterized in the central Ribeira belt (Machado et al., 1996; Heilbron and Machado, 2003). The deformational overprint is characterized by a combination of dextral subvertical mylonite zones and intervening tracts of normal (D3) folding. Granite emplacement is typically associated with the mylonite zones, frequently foliated only along their margins, retaining often magmatic flow textures in central domains. The M2 metamorphic overprint is widespread in the Costeiro Domain, and its age is given by U-Pb ages of monazite or titanite and by lower intercepts of zircon discordia lines (Machado et al., 1996; Heilbron and Machado, 2003; Heilbron et al., 2008). This event was correlated with the docking of the Cabo Frio terrane (Heilbron et al., 2003), where Schmitt et al. (2004) characterized an orogenic imprint at *ca*. 520 Ma.

2.5. The post-collisional phase and the leucogranite suites

The emplacement of post-orogenic granites subsequent to the 530-520 Ma orogenic episode resulted in diapiric stocks and plutons defining elliptical outcrop patterns. These are closely associated with the emplacement of aplite and pegmatite dykes and sheets with sharp contacts relative to the country rocks. Concentrations of xenoliths are frequently observed. All of these features suggest magmatic emplacement at relatively shallow crustal levels.

In a recent geologic mapping by the CPRM- Brazilian Geological Survey (i.e. Valeriano et al., in press; Tupinambá et al., in press), the post-collisional granites have been formally separated into the older Suruí and the younger Nova Friburgo suites, based on geochronological, compositional and structural criteria.

The Suruí suite is represented by the Pedra Branca batholith (Porto and Figueiredo, 1996), a 150 km^2 intrusive complex in west Rio city, and by the Suruí Granite, an elliptical 60 km^2 pluton of megaporphyric granite located NW of the Guanabara Bay. Both the Pedra Branca and Suruí granites display a predominant porphyritic texture with magmatic flow foliation frequently superimposed by weak ductile deformation.

The Pedra Branca Complex is represented predominantly by monzogranites and syenogranites, but also includes rocks such as gabbro, quartz-diorite and tonalite, consistent with an expanded metaluminous calc-alkaline series (Porto and Figueiredo, 1996). The Pedra Branca Granite was previously dated by Heilbron and Machado (2003) by U-Pb at 513 + 5 Ma.

The Nova Friburgo suite comprises a large number of relatively small intrusive complexes including the Paraty, Mambucaba, Mangaratiba, Favela, Andorinha, Frades, Nova Friburgo and Sana bodies, that occur along with smaller stocks and abundant dykes cross-cutting all granitic/gneissic geological units. They are mostly equigranular leucocratic titanite-bearing calc-alkaline I-type granites (Junho et al., 1987). Foliation due to magmatic flow is very frequent. The lack of any ductile deformation and characteristically sharp and planar contacts with enclosing rocks point to relatively shallow depths of intrusion. The Favela and Mangaratiba granites, located respectively at and 100 km west of Rio de Janeiro city, were previously dated by U-Pb at 492+-15 Ma and 482+- 6 Ma respectively (Machado et al., 1996; Heilbron and Machado, 2003).

In the northern Ribeira belt, and its northerly continuation into the Araçuaí belt, the post-collisional magmatism is represented by a large number of diapiric intrusive zoned complexes, frequently bimodal, including the Mimoso do Sul, Santa Angélica, Várzea Alegre and Aimorés complexes. These complexes display a similar range of radiometric ages (De Campos et al., 2004), that will be discussed below along with the new results.

Previous U-Pb data reported for the post-collisional granites in the Rio de Janeiro State indicate a ~30 Ma span in ages (between 513 and 480 Ma) within Cambro-Ordovician time for post-collisional magmatism (Machado et al., 1996; Heilbron and Machado, 2003). Within the northern section of the Ribeira belt located in the Espírito Santo State, Sollner et al. (2000) have also reported a similar range of U-Pb ages for the post-tectonic diapiric intrusive complexes. These previous U-Pb results will be discussed together with the new data presented here.

3. Analytical procedure

3.1. Sampling

Samples from the Suruí, Sana, Nova Friburgo and Frades intrusions and one pegmatite dyke were collected for zircon extraction. These four sampling sites are distributed along a 100 km segment of the central Ribeira belt in the Rio de Janeiro State. Detailed descriptions of sampling localities are provided with the results.

3.2. Sample preparation

The preparation of samples was carried out at the LGPA Laboratory, UERJ - Rio de Janeiro State University, where utmost care was taken in order to avoid cross contamination between samples. Concentration of heavy minerals involved jaw-crushing, disk-milling, manual panning and Frantz magnetic separation. Grains free of inclusions and fractures were selected from the least magnetic fractions. The selected grains were then placed within epoxy resin mounts and subsequently ground to expose the largest surface areas. This was followed by a polishing stage involving alumina oxide powder, and final polishing by diamond pastes using a mechanical disc table.

3.3. U-Pb LA-MC-ICPMS analysis

The LA-MC-ICP-MS U-Pb analyses were conducted at the Radiogenic Isotope Facility within the Department of Earth and Atmospheric Sciences, University of Alberta (Edmonton, Canada). A detailed description of the analytical method employed here is given by Simonetti et al. (2005, 2008). The Nu Plasma multi-collector-ICP-MS instrument is equipped with three ion counters and twelve Faraday cups and is coupled to a UP213 Nd:YAG laser

Fig. 3. Common textural varieties of the post-collisional granite suites: a) magmatic flow registered by tabular megacrysts of the porphyritic granite of the Frades Pluton at one of the Três Picos summits (photo: Marcelo Ferrasolli); b) contact between the porphyritic Suruí Granite and cross-cutting pegmatite dyke; c) homogeneous equigranular facies of the leucocratic Sana Granite (photo: Julio Almeida); d) K-feldspar megacrysts of the porphyritic granite of the Nova Friburgo Pluton at the Caledônia Massif. Hammer head for scale (10 cm).

ablation system (New Wave Research-ESI). A laser beam diameter of 40 microns was used with corresponding energy density (fluence) of ~2–3 J cm^{-2} and repetition rate of 4 Hz. Ablated material is transported towards the torch region of the MC-ICP-MS instrument using He carrier gas (1.0 L/min). All analyses were carried out in static multi-collection mode. The acquisition of 30 isotope ratios (1 s integration) occurred following measurement of the background (blank) ion signals for 30 s. Instrumental mass bias is corrected using the measured $^{205}Tl/^{203}Tl$ ratio (certified = 2.3871) for a 2.5 ppb solution (2% HNO_3) of the certified NIST SRM 997 Thallium isotopic standard that is aspirated simultaneously during lasering via a DSN-100 desolvating nebulizer (Nu Instruments Ltd) that is 'Y'-connected to the laser ablation sample-out line. LIEF (laser induced elemental fractionation) was monitored via the 'standard-sample' bracketing method using LH94-15 zircon (Simonetti et al., 2005) and the Khan titanite (Simonetti et al., 2006) in-house external standards.

4. Results

Analytical results are shown in Appendix A. The calculation of ages and concordia plots were performed using the Isoplot software v. 3.0 (Ludwig, 2003). In all concordia diagrams the individual data-point error ellipses in the U-Pb plots represent uncertainties reported at the 2 sigma level. The new results are reported below in geographic order, from west to east (Fig. 2).

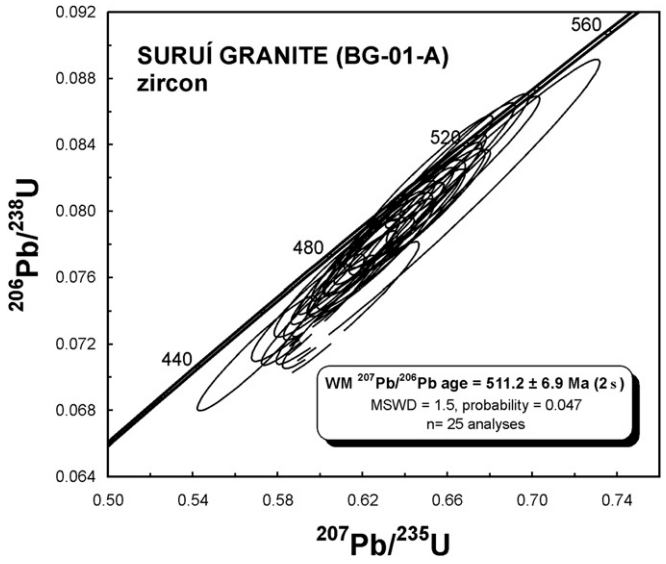

Fig. 4. Concordia diagram for 25 zircon grains from the Suruí Granite (sample BG-01-A), with a weighted average of $^{206}Pb/^{207}Pb$ ages at 511.2 +- 6.9 Ma.

4.1. Suruí Granite (sample BG-01-A)

Sample BG-01-A was collected at the Suruí Quarry, located north of Guanabara Bay along the highway BR-116 (22.66038°S, 43.11415°W). In this outcrop, the Suruí Granite displays its typical texture of oriented K-feldspar megacrysts as a result of by magmatic flow. The megacrysts exhibit slight lattice deformation, indicated by undulose extinction when observed in thin section under cross-polarized light, but not enough to render the granite an "augen" fabric. The Suruí Granite is discordantly cross-cut by an assemblage of pegmatite and pink-colored, fine-grained isotropic granite (the Andorinha Granite) and leucogranite aplitic veins.

Twenty four grains were analyzed, most colorless prismatic (3:1 to 8:1 aspect ratio), and yielded ages with degrees of discordance between 0.8% and 12.5% (Fig. 4). The most concordant grain (0.8% discordance) yielded a $^{207}Pb/^{206}Pb$ age of 510 ± 25 Ma and similar age on tip. The weighted average of the twenty four $^{207}Pb/^{206}Pb$ ages is 511.2 ± 6.9 Ma (MSWD = 1.5), interpreted as the best estimate for the age of the Suruí Granite.

4.2. Andorinha Granite composite dyke intruding the Suruí Granite (sample BG-01-A)

A composite pegmatite-granite dyke of 2m thickness intrudes the Suruí Granite. The pegmatite grades towards the central zone of the dyke into an equigranular, fine-grained granite, regionally referred as the Andorinha Granite; both display undeformed igneous textures.

Zircon grains from the pegmatite are colorless, with either equidimensional or long prismatic (5:1 aspect ratio) habits. A set of 16 grains was analyzed yielding variable degrees of discordance between 1% and 17% (with the exception of one grain – 43%; Appendix A). The interpreted age for the pegmatitic border of the dyke (Fig. 5) is 497.7 ± 9.2 Ma (MSWD = 0.16) and it was based on the concordia age calculated for the three most concordant grains (#s 2, 13, 14 - 1–2% discordant).

4.3. Frades Granite (sample TP-137)

Sample TP-137 was retrieved from the Três Picos pluton, one of several granite stocks of the Frades Complex, located in the Serra dos Órgãos mountains north of Rio de Janeiro city, between the of Teresópolis and Nova Friburgo towns. The sample investigated here was collected from the middle summit of the Três Picos ("three

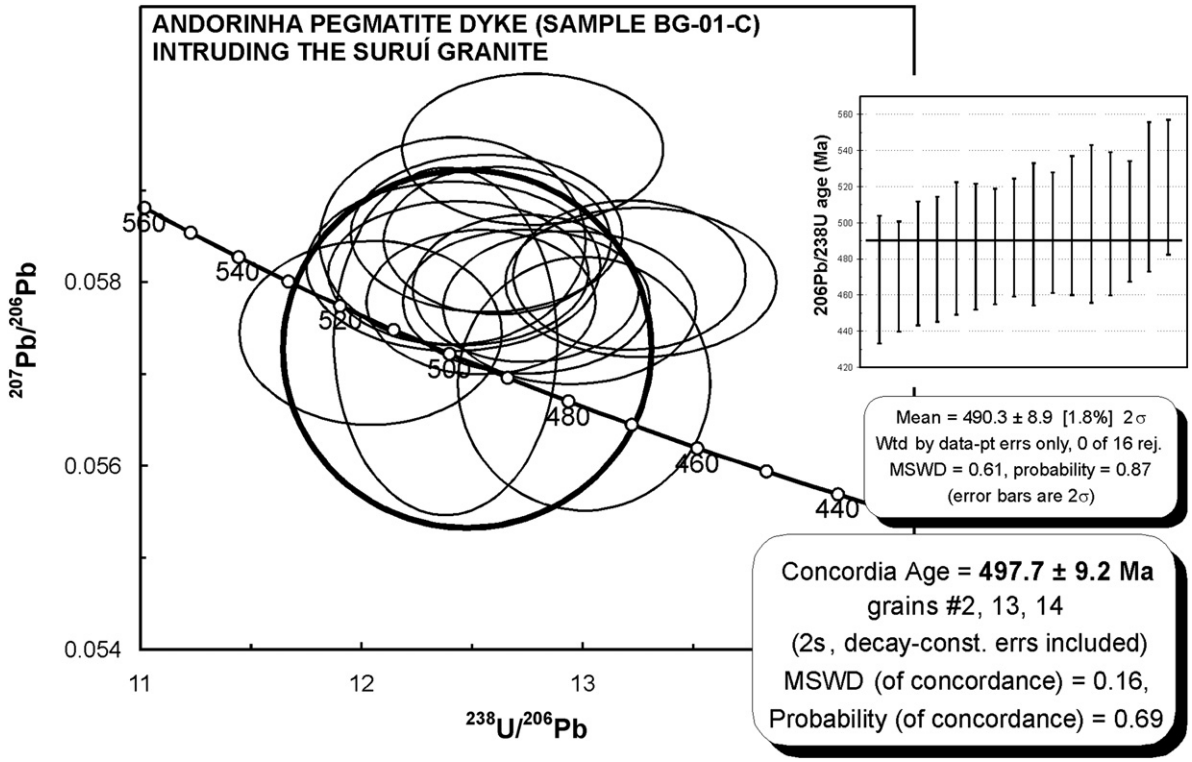

Fig. 5. Tera-Wasserburg plot exhibiting U-Pb results for the pegmatitic facies of the Andorinha Granite (Sample BG-01-A), intruding the Suruí Granite.

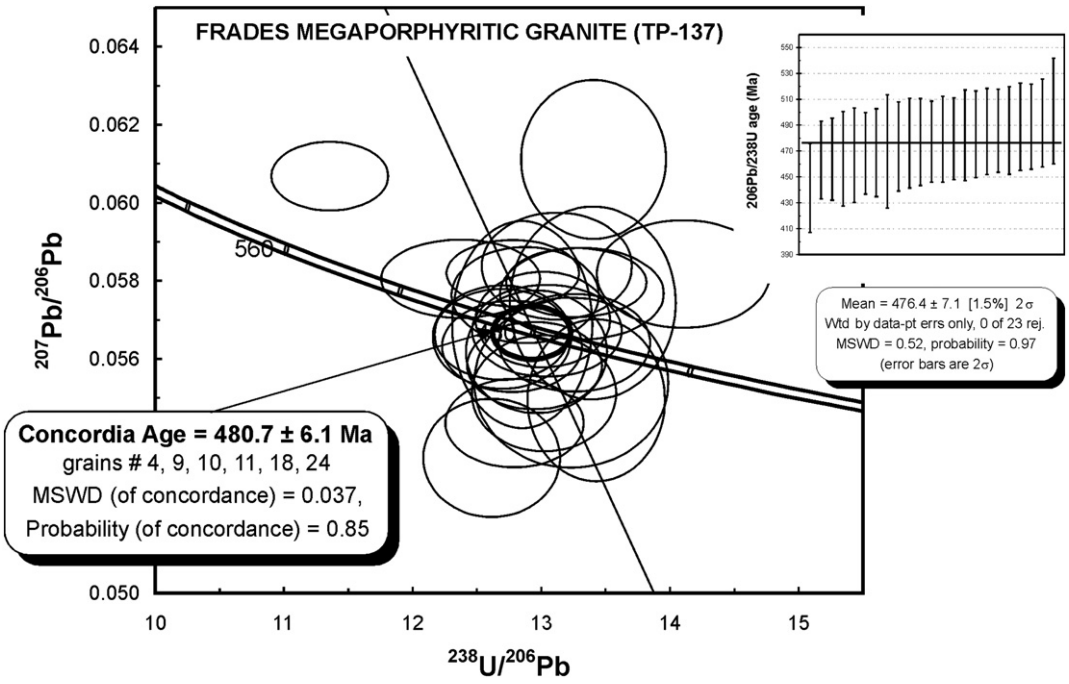

Fig. 6. Tera-Wasserburg diagram illustrating the U-Pb results for zircons analyzed from the Frades Granite.

peaks") mountains at 2144 m above sea level (22.342302°S – 42.727678°W). Oriented tabular K-feldspar megacrysts impart a conspicuous magmatic flow foliation to the rock (Fig. 3a).

Zircon grains from this sample are colorless to yellow equidimensional or short prismatic crystals, with up to 3:1 aspect ratio. A total of 24 zircon grains were analyzed and yielded a weighted mean $^{206}Pb/^{238}U$ age of 476.4 ± 6.9 Ma (MSWD = 0.5). The best estimate for the crystallization age of the Frades Granite (Fig. 6) is 480.7 ± 6.1 Ma as defined by the concordia age based on the 6 most concordant grains (#4, 9, 10, 11, 18, 24).

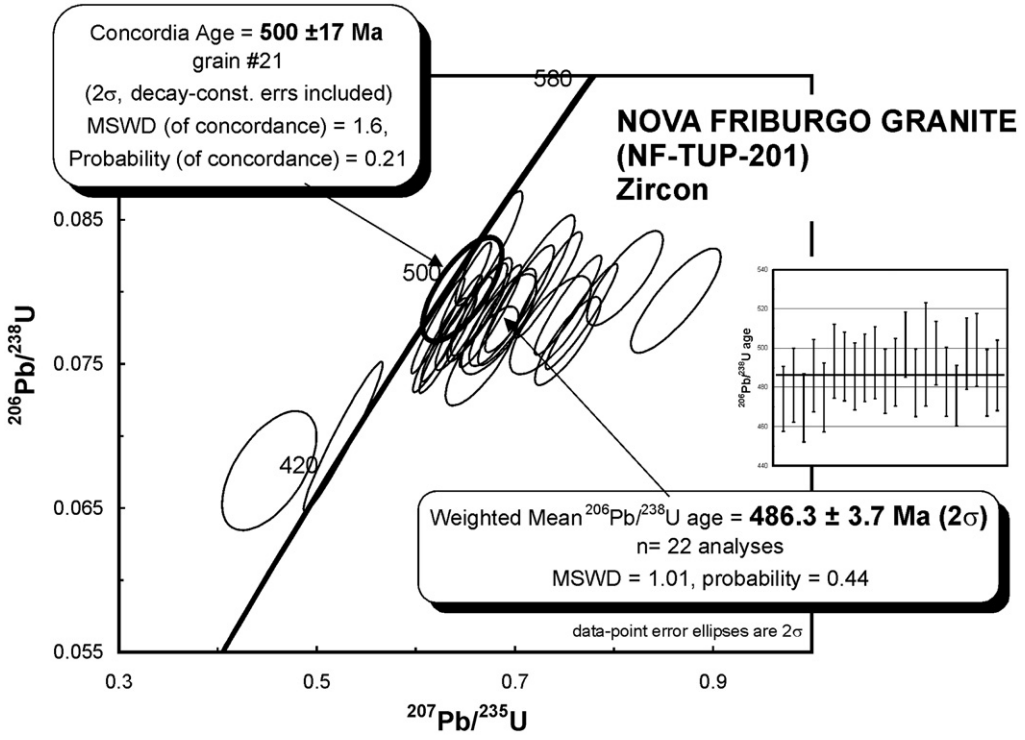

Fig. 7. Concordia plot of zircon analyses from the Nova Friburgo Granite. Inset of distribution plot shows the individual $^{206}Pb/^{238}U$ ages and weighted mean age.

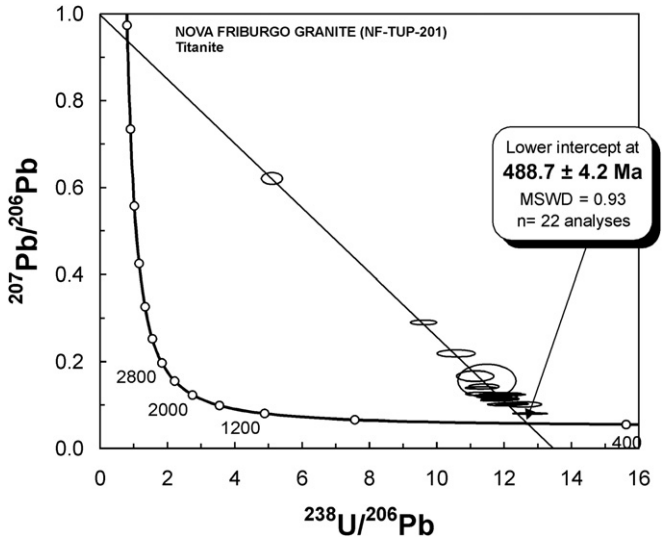

Fig. 8. Tera-Wasserburg diagram illustrating the U-Pb data for titanite obtained from the Nova Friburgo Granite.

4.4. Nova Friburgo granite (sample NF-TUP-201)

Sample NF-TUP-201 was collected at the Caledônia Mountain, 6 km SW of the town of Nova Friburgo (22.332626°S – 42.572560°W). The rocks from the Nova Friburgo Pluton exhibit predominantly a porphyritic texture. The sample investigated here is a biotite-titanite porphyritic granite containing microcline megacrysts hosted by a coarse-grained matrix of syenogranitic composition. Titanite is an essential mineral and occurs as euhedral and subhedral crystals associated with biotite and opaque minerals (e.g., ilmenite).

Zircons from this sample are yellowish to colorless prismatic grains (3:1 to 6:1 aspect ratios). A set of 24 zircons was analyzed (Fig. 7), with the most concordant grain (#21, 0.4% discordant) yielding a $^{207}Pb/^{206}Pb$ age of 500 ± 17 Ma. The weighted mean of twenty two $^{206}Pb/^{238}U$ ages of 486.3 ± 3.7 Ma (MSWD = 1.01), however, is interpreted as the best estimate for the crystallization age of the Nova Friburgo Granite (Fig. 8). A total of 26 titanite grains from the same sample was also analyzed. Twenty two of these grains define an inverse discordia line (Tera and Wasserburg, 1972) with a lower intercept at 488.7 ± 4.2 Ma (MSWD = 0.93), and weighted mean $^{206}Pb/^{238}U$ age of 488.3 ± 3.7 Ma (n = 22 grains; MSWD = 0.84).

4.5. Sana Granite (sample JA-FM-02)

Among the several intrusive complexes from the studied area, the Sana Granite is one that has the largest outcrop area, with numerous small stocks of kilometer diameter or smaller intruding the paragneisses of the São Fidélis Complex.

This individual pluton of the Sana Granite has a diameter of 18 km. It comprises equigranular biotite leucogranite, mostly with near isotropic texture or faint to well developed magmatic flow foliation given by preferred orientation of biotite, and minor porphyritic facies. Mineralogy is constituted by quartz (35%), microcline (30%), plagioclase (10%), perthitic orthoclase (7%), and minor biotite, allanite and opaque minerals. Zircon, apatite and titanite are accessory, with chlorite, muscovite and saussurite occurring as alteration products.

Sample JA-FM-02 was collected in a boulder field in the central portion of the pluton proximal to road RJ-142 between the town of Casemiro de Abreu and Sana village. The sample is from a boulder with diameter of 16 m (22.304280°S, 42.171085°W).

Zircons from this sample are all colorless, ranging from needle shaped to equidimensional crystals. A set of 24 zircon grains were

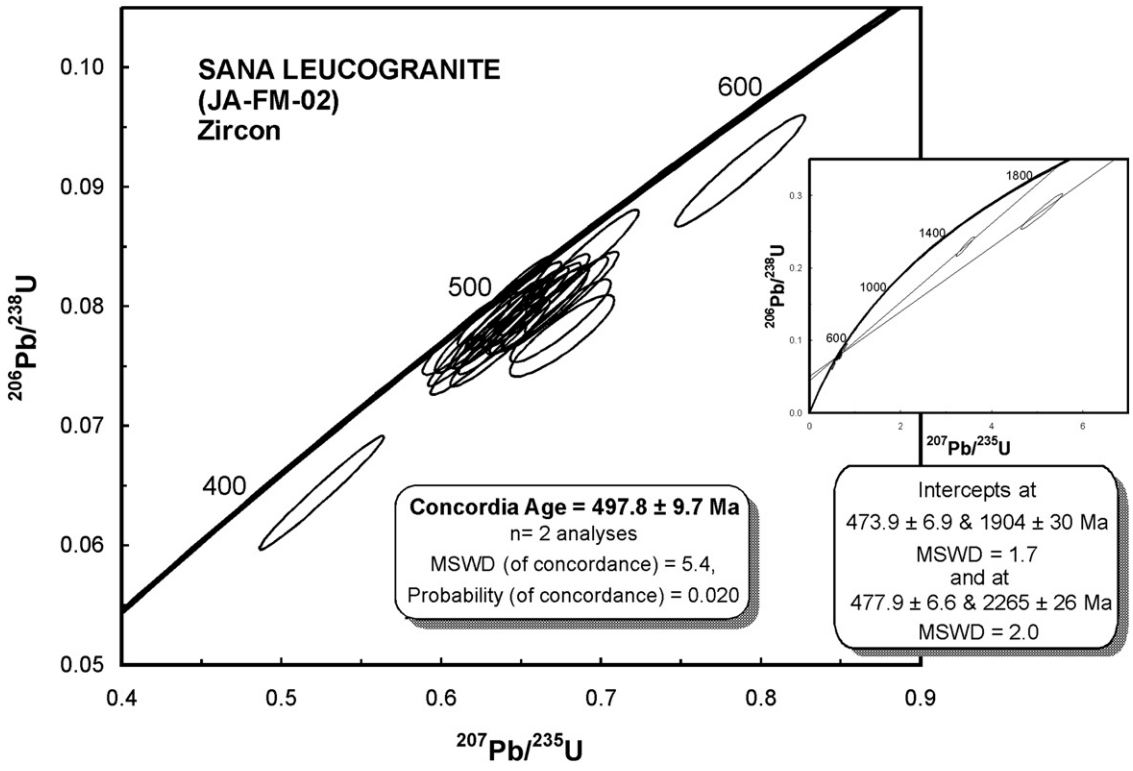

Fig. 9. Concordia plot of the Sana Granite.(The inset diagram represents two inherited grains with Paleoproterozoic upper intercept ages, out of scale from the main diagram).

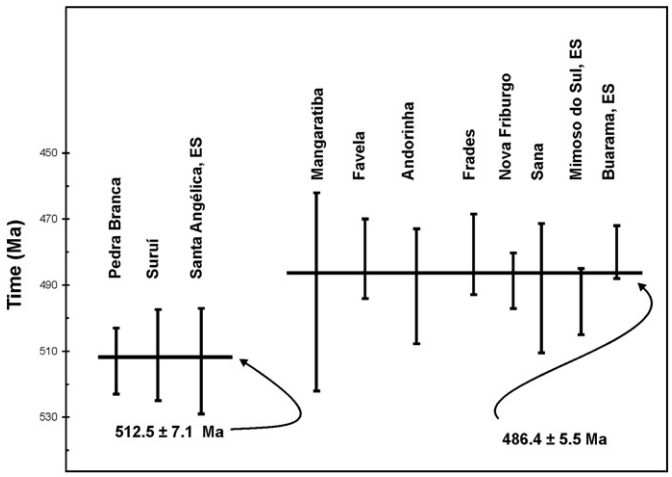

Fig. 10. Distribution of U-Pb ages of post-collisional granites showing two main pulses of magmatic activity at *ca.* 513 Ma and at *ca.* 486 Ma, each organized from west to east.

analyzed yielding a range of discordance, between −2% and 30% (Appendix A). Two short prismatic colorless grains (#12 and #23) yield Paleoproterozoic $^{207}Pb/^{206}Pb$ ages, and they were interpreted as inherited (Fig. 9). The remaining 22 grains of prismatic habit (3:1 to 6:1 aspect ratio) yield a weighted mean $^{206}Pb/^{238}U$ age of 490.9 ± 9.8 Ma (MSWD = 1.4), which is interpreted as the best estimate for the crystallization of the Sana Granite.

5. Discussion

A summary of the new and previously published U-Pb ages of post-collisional granites in Rio de Janeiro and Espírito Santos States are listed in Table 1, from southwest to northeast along the central-northern Ribeira belt.

The ages of the Suruí Granite (511 ± 7 Ma) and cross-cutting Andorinha pegmatite dyke (490 ± 9 Ma) agree very well with those previously reported within the central Ribeira belt for the Pedra Branca Granite (513 ± 5 Ma) and the cross-cutting Favela Granite dyke (483 ± 2 Ma) in Bangu, west end of Rio de Janeiro city (Heilbron and Machado, 2003). This younger and last phase of Ordovician granite production also coincides (within associated uncertainties) with the previously reported age of 480 ± 8 Ma for the titanite-bearing Mangaratiba Granite, located on the coast to the west of Rio de Janeiro (Machado et al., 1996).

The compilation of 11 previous and new U-Pb ages listed in Table 1, which represent ages for plutonism distributed almost 400 km along the orogen's strike, indicate a bimodal age distribution (Fig. 10). This agrees very well with the two main phases of magmatic activity previously identified on the basis of geological criteria. The older Cambrian magmatic pulse dated at 512.5 ± 7.1 Ma is defined by the weighted mean ages for the Pedra Branca (Heilbron and Machado, 2003), Suruí (this work) and Buarama plutons (Espírito Santo State, Söllner et al., 2000). The younger Ordovician magmatic phase dated at 486.4 ± 5.5 Ma is defined by the weighted mean ages for the Mangaratiba (Machado et al., 1996), Favela (Heilbron and Machado, 2003), Três Picos, Nova Friburgo, and Sana plutons, and by the undeformed and pegmatite dyke (this work; Fig. 12).

In a broader geological context, the ages listed in Table 1 correlate well with the available data regarding the post-collisional magmatism in the northern Ribeira belt and, more to the north, in the Araçuaí belt. The bimodal age distribution (~513 Ma and ~486 Ma) of the post-collisional magmatism reported here for the central Ribeira belt shows a remarkable match with the observation that the 480 ± 4 Ma Buarama titanite-bearing granite, in the northern Ribeira belt (Espírito Santo State), contains enclaves

Table 1
Summary of U-Pb ages of post-orogenic granites from the Ribeira belt in the Rio de Janeiro and Espírito Santo states, southeast Brazil. References: 1- this work; 2- Sollner et al. (1987); 3- Machado et al. (1996); 4- Söllner et al. (2000); 5- Heilbron and Machado (2003).

Post-collisional intrusion	Age (Ma)	Method and age detail
Andorinha Granite, pegmatitic facies (1)	490.3 ± 8.7	LA-ICPMS- weighted av. (n = 16) of $^{206}Pb/^{238}U$ zircon ages
Sana Granite (1)	490.9 ± 9.8	LA-ICPMS, weighted av. (n = 22) of $^{206}Pb/^{238}U$ zircon ages
Nova Friburgo Granite (1)	488.7 ± 4.2	LA-ICPMS, titanite lower intercept
Frades Granite (1)	480.7 ± 6.1	LA-ICPMS, zircon concordia age
Favela Granite (5)	482 ± 6	LA-ICPMS - weighted average of 2 concordant zircon grains
Mangaratiba Granite (3)	492 ± 15	ID-TIMS, titanite upper intercept
Suruí Granite (1)	511.2 ± 6.9	LA-ICPMS, weighted average (n = 25) of $^{207}Pb/^{206}Pb$ ages
Pedra Branca Granite (5)	513 ± 5	ID-TIMS, zircon upper intercept
SA51- Santa Angélica megaporphyritic allanite granite, Espírito Santo state (2)	513 ± 8	ID-TIMS, zircon upper intercept
MS11 monzosyenite, near Mimoso do Sul, E spírito Santo state (4)	495 ± 5	ID-TIMS zircon
BU11 Buarama outer rim titanite granite (4)	480 ± 4	ID-TIMS zircon

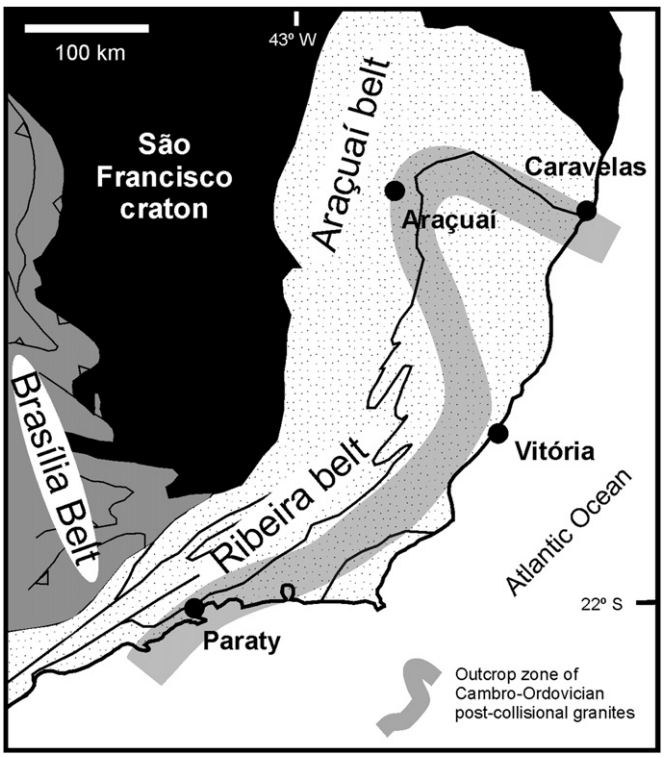

Fig. 11. Sinuous Cambro-Ordovician granite belt (gray band) stitching the Araçuaí and Ribeira orogens. It probably marks a zone of post-collisional lithospheric thinning due either to subducted slab break off or to orogenic collapse of overthickened hot continental crust.

of the 513 ± 8 Ma allanite-bearing Santa Angélica Granite (Söllner et al., 1987, 2000).

In the Araçuaí belt, the continuation to the north of the Mantiqueira Province, the post-collisional magmatism is represented by numerous large and small biotite granite, charnockite and/or norite intrusions. These are classified by Pedrosa-Soares et al. (2008) in two different magmatic suites: the G4 (S-type) suite spans between 530 and 500 Ma; and the G5 (I-type) suite defines a slightly younger age span, from 520 to 490 Ma. Although broadly overlapping in time, two pulses of post-collisional magmatism seem to have taken place within the Araçuaí belt.

Two geodynamic models are proposed as triggering mechanisms for the Cambrian-Ordovician magmatism: post-collisional break off of subducted oceanic lithosphere (Söllner et al., 1987, 2000), or an extensional collapse of overthickened crust (Heilbron and Machado, 2003; Pedrosa Soares et al., 2008). Both models emphasize the melting of ascending asthenospheric mantle and the interaction of melt with lower continental crust. In fact, chemically bimodal zoned elliptical diapiric intrusions of the northern Ribeira belt are interpreted by De Campos et al. (2004) as the product of interaction between mantle-derived magmas and partial melting of the deep crust.

The geographic distribution of the Cambro-Ordovician post-collisional magmatism broadly defines a long and sinuous belt about 50 km wide. In map view (Fig. 11), the post-collisional granite belt extends from Caravelas at the seashore to Araçuaí, turning sharply to SSE towards Vitória, where it again deflects to SW, towards Paraty. This Cambrian-Ordovician post-collisional granite belt marks the locus of sub-lithospheric thermal erosion, either caused by slab detachment and/or extensional collapse of the orogen.

From the southern Ribeira belt (southern São Paulo and Paraná States) to the southernmost segments of the Mantiqueira Province (southern Brazil and Uruguay), any Cambrian-Ordovician magmatism is apparently absent. The youngest recorded magmatism within these regions dates at least 535 Ma (Camaquã volcanism) or older, *ca* 564 as in the case of São Paulo State (Leite et al., 1997; Janasi et al., 2001). The Cambrian-Ordovician magmatism documented here for the central and northern regions of the Ribeira belt post-dates even the *ca*. 530 Ma inversion of the late-Ediacaran (560-540 Ma) Eleutério, Castro, Itajaí, Camaquã and other Brasiliano foreland and intermontane sedimentary basins of the southern Mantiqueira Province (Almeida et al., 2008).

6. Conclusions

The age determinations obtained here for the terminal phase of Brasiliano magmatism in the central Ribeira belt are: 511.2 ± 6.9 Ma (zircon) for the Suruí Granite; 490.3 ± 8.7 Ma (zircon) for a cross-cutting pegmatite dyke from the same outcrop; 480.7 ± 6.1 Ma (zircon) for the Frades Granite; 488.7 ± 4.2 Ma (titanite) for the Nova Friburgo Granite; and 490.9 ± 9.8 Ma (zircon) for the Sana Granite.

These new results together with the U-Pb ages compiled from the literature for the post-orogenic intrusions, distributed along almost 400 km of the orogen's strike in Rio de Janeiro and Espírito Santo States, reinforce the idea of two distinct magmatic pulses: an older Cambrian one at *ca*. 513 Ma (Pedra Branca, Suruí and Buarama granites) and a younger Ordovician granite pulse at *ca*. 486 Ma (Mangaratiba, Favela, Frades, Nova Friburgo, Sana plutons and pegmatite dyke). The Cambrian pulse post-dates the end of the first and main collisional phase of the Ribeira belt by *ca*. 35 m.y. It also post-dates the onset of the second collisional episode by *ca*. 20 m.y. The late-Ordovician magmatic pulse post-dates the end of the second collisional episode by *ca*. 25 m.y.

In map view, the alignment of the post-collisional plutons and stocks depicts a sinuous belt running along the eroded roots of central/northern Ribeira and Araçuaí belts. This granite belt probably marks the zone where preferential heating and melting of lower continental crust took place, either caused by breaking off of subducted slab, or by the extensional collapse of hot, overthickened continental crust.

Acknowledgments

The CPRM – Brazilian Geological Survey is acknowledged for financial support for field work and analyses.

Appendix A

Analytical U-Pb results. Lines printed in bold refer to the most concordant grain(s) of each sample.

Grain #	^{206}Pb cps	^{206}Pb/^{204}Pb	^{207}Pb/^{206}Pb	2s error	^{207}Pb/^{235}U	2s error	^{206}Pb/^{238}U	2s error	^{207}Pb/^{206}Pb Age (Ma)	2s error	^{206}Pb/^{238}U Age (Ma)	2s error	discord. %
BG-01-A - Suruí Granite–Zircon													
1	256993	infinite	0.05780	0.00066	0.6681	0.0248	0.0833	0.0031	522	±25	516	±19	1.2
2	133126	infinite	0.05760	0.00069	0.6415	0.0285	0.0799	0.0035	514	±26	495	±22	3.7
3	271093	infinite	0.05826	0.00065	0.6502	0.0246	0.0800	0.0030	539	±24	496	±19	8.0
4	202201	infinite	0.05792	0.00067	0.6674	0.0296	0.0825	0.0036	527	±25	511	±22	3.0
5	102239	infinite	0.05776	0.00081	0.6336	0.0285	0.0783	0.0034	521	±31	486	±21	6.6
6	166440	infinite	0.05732	0.00062	0.6327	0.0250	0.0788	0.0031	504	±24	489	±19	2.9
7	313304	infinite	0.05748	0.00060	0.6194	0.0243	0.0775	0.0030	510	±23	481	±19	5.6
8	136957	infinite	0.05693	0.00068	0.5703	0.0230	0.0714	0.0028	489	±26	445	±18	9.0
9	89465	29822	0.05823	0.00107	0.6557	0.0623	0.0800	0.0075	538	±40	496	±47	7.9
10	195648	infinite	0.05791	0.00065	0.5993	0.0220	0.0740	0.0027	526	±25	460	±17	12.5
11	66915	infinite	0.05684	0.00081	0.6075	0.0237	0.0759	0.0029	485	±31	472	±18	2.8
12	65789	infinite	0.05727	0.00076	0.6145	0.0263	0.0743	0.0031	502	±29	462	±19	7.9
13	164090	infinite	0.05741	0.00066	0.6261	0.0264	0.0777	0.0033	507	±25	483	±20	4.9
14	88634	infinite	0.05696	0.00074	0.6449	0.0274	0.0805	0.0034	490	±29	499	±21	−1.9
15	78884	infinite	0.05689	0.00067	0.6614	0.0250	0.0828	0.0031	487	±26	513	±19	−5.2
16	99197	infinite	0.05733	0.00079	0.5944	0.0218	0.0742	0.0026	504	±30	461	±16	8.5
17	61790	infinite	0.05737	0.00085	0.6241	0.0244	0.0772	0.0029	506	±33	479	±18	5.3
18	**994127**	**infinite**	**0.05749**	**0.00067**	**0.6488**	**0.0267**	**0.0817**	**0.0033**	**510**	**±25**	**506**	**±21**	**0.8**
18b	1408303	infinite	0.05818	0.00087	0.6458	0.0261	0.0800	0.0031	537	±33	496	±19	7.6
19	57907	infinite	0.05741	0.00096	0.6404	0.0230	0.0798	0.0027	507	±37	495	±16	2.4
20	117432	infinite	0.05735	0.00062	0.6119	0.0209	0.0764	0.0026	505	±24	474	±16	6.1

(*continued on next page*)

(*continued*)

Grain #	^{206}Pb cps	^{206}Pb/^{204}Pb	^{207}Pb/^{206}Pb	2s error	^{207}Pb/^{235}U	2s error	^{206}Pb/^{238}U	2s error	^{207}Pb/^{206}Pb Age (Ma)	2s error	^{206}Pb/^{238}U Age (Ma)	2s error	discord. %
21	167706	infinite	0.05698	0.00066	0.6251	0.0239	0.0782	0.0030	491	±26	485	±18	1.1
22	126241	infinite	0.05726	0.00077	0.6272	0.0211	0.0780	0.0025	501	±30	484	±16	3.4
23	483339	infinite	0.05831	0.00061	0.6187	0.0211	0.0764	0.0026	542	±23	475	±16	12.4
24	170488	infinite	0.05743	0.00071	0.6098	0.0221	0.0755	0.0027	508	±27	469	±17	7.6
BG-01-C - Andorinha pegmatite Zircon													
1	135705	infinite	0.05772	0.00068	0.6301	0.0231	12.9422	0.4675	519	±26	480	±17	7.6
2	48739	infinite	0.05745	0.00082	0.6747	0.0280	12.0420	0.4844	**509**	**±31**	**514**	**±21**	**−1.1**
3	97786	infinite	0.05817	0.00075	0.6592	0.0293	12.4165	0.5430	536	±28	499	±22	6.9
4	95445	23861	0.05845	0.00092	0.6657	0.0276	12.4128	0.4914	547	±34	499	±20	8.6
5	118517	infinite	0.05800	0.00066	0.6178	0.0236	13.2643	0.5007	530	±25	469	±18	11.5
6	112514	infinite	0.05778	0.00064	0.6544	0.0223	12.5414	0.4229	521	±24	495	±17	5.2
7	173825	infinite	0.05810	0.00064	0.6570	0.0256	12.4379	0.4802	533	±24	499	±19	6.5
8	235983	infinite	0.05808	0.00067	0.6205	0.0205	13.2132	0.4292	533	±25	470	±15	11.7
9	139856	infinite	0.05853	0.00070	0.6605	0.0267	12.5659	0.5017	550	±26	494	±20	10.2
10	233182	infinite	0.05793	0.00065	0.6382	0.0212	12.7446	0.4185	527	±25	487	±16	7.6
11	243577	infinite	0.06923	0.00280	0.8175	0.0434	11.9101	0.4276	905	±83	520	±19	42.6
12	229608	infinite	0.05779	0.00064	0.6368	0.0230	12.7465	0.4561	522	±24	487	±17	6.7
13	**486111**	**16204**	**0.05690**	**0.00113**	**0.6102**	**0.0242**	**13.0065**	**0.4661**	**487**	**±44**	**477**	**±17**	**2.0**
14	**261744**	**6888**	**0.05735**	**0.00155**	**0.6533**	**0.0272**	**12.3808**	**0.4128**	**505**	**±59**	**501**	**±17**	**0.9**
15	214346	infinite	0.05845	0.00066	0.6521	0.0219	12.6151	0.4195	547	±25	492	±16	10.1
16	185063	infinite	0.05945	0.00067	0.6663	0.0254	12.7741	0.4824	583	±25	486	±18	16.7
TP-137 - Três Picos Granite - Zircon													
1	17545	infinite	0.0535	0.0012	0.5979	0.0241	12.6142	0.4342	348	52	492	17	−41.1
2	36722	infinite	0.0577	0.0010	0.6135	0.0253	13.3153	0.5202	517	37	467	18	9.8
3	30358	infinite	0.0558	0.0009	0.6136	0.0218	12.9480	0.4275	445	36	480	16	−7.7
4	**25386**	**infinite**	**0.0570**	**0.0010**	**0.6216**	**0.0223**	**13.0117**	**0.4266**	**492**	**39**	**477**	**16**	**2.9**
5	81926	infinite	0.0582	0.0007	0.6415	0.0216	12.7788	0.4212	537	26	486	16	9.6
6	126286	infinite	0.0580	0.0007	0.6141	0.0212	13.2725	0.4465	528	27	468	16	11.3
7	33874	infinite	0.0563	0.0010	0.6243	0.0234	12.7733	0.4443	465	38	486	17	−4.5
8	19148	infinite	0.0554	0.0018	0.5997	0.0334	13.2323	0.6163	428	72	470	22	−9.7
9	**25428**	**infinite**	**0.0566**	**0.0010**	**0.6378**	**0.0231**	**12.6921**	**0.4271**	**477**	**37**	**489**	**16**	**−2.5**
10	**32093**	**infinite**	**0.0567**	**0.0010**	**0.6129**	**0.0239**	**13.0429**	**0.4750**	**481**	**38**	**476**	**17**	**0.9**
11	**18824**	**infinite**	**0.0564**	**0.0010**	**0.5993**	**0.0236**	**13.2575**	**0.4809**	**469**	**40**	**469**	**17**	**0.0**
12	215550	infinite	0.0607	0.0007	0.7491	0.0250	11.3562	0.3713	628	26	544	18	13.4
13	16546	infinite	0.0544	0.0009	0.6032	0.0223	12.7919	0.4387	386	38	485	17	−25.8
14	28234	infinite	0.0576	0.0010	0.6429	0.0251	12.8750	0.4681	516	38	482	18	6.5
15	58065	infinite	0.0581	0.0008	0.6676	0.0280	12.3732	0.5036	532	31	501	20	5.8
16	16454	infinite	0.0574	0.0020	0.6170	0.0320	13.3997	0.5276	508	77	464	18	8.7
17	15877	infinite	0.0551	0.0012	0.6118	0.0247	13.0210	0.4583	417	49	477	17	−14.4
18	**22142**	**infinite**	**0.0566**	**0.0011**	**0.6371**	**0.0244**	**12.6955**	**0.4396**	**474**	**42**	**489**	**17**	**−3.0**
19	19482	infinite	0.0611	0.0017	0.6579	0.0281	13.4057	0.4599	643	59	464	16	27.9
20	33323	infinite	0.0582	0.0011	0.5904	0.0250	14.1031	0.5498	536	42	442	17	17.7
21	14441	infinite	0.0549	0.0017	0.5837	0.0255	13.4268	0.4362	410	69	463	15	−13.0
22	15039	infinite	0.0562	0.0013	0.6216	0.0250	12.9621	0.4482	460	51	479	17	−4.2
23	27756	infinite	0.0584	0.0011	0.6321	0.0252	13.1209	0.4767	544	42	473	17	12.9
24	**17344**	**infinite**	**0.0569**	**0.0022**	**0.6395**	**0.0323**	**12.8517**	**0.4449**	**487**	**84**	**483**	**17**	**0.8**
NF-TUP-201 - Nova Friburgo Granite - Zircon													
1	138857	infinite	0.05805	0.00072	0.6243	0.0223	0.0763	0.0027	532	27	474	17	10.9
2	100541	infinite	0.05770	0.00068	0.6361	0.0251	0.0775	0.0030	518	26	481	19	7.2
3	95874	infinite	0.06348	0.00174	0.6668	0.0301	0.0755	0.0028	724	58	469	17	35.2
4	165943	infinite	0.06961	0.00085	0.7674	0.0297	0.0783	0.0030	917	25	486	18	47.0
5	81768	infinite	0.05768	0.00071	0.6324	0.0238	0.0764	0.0028	518	27	475	18	8.3
6	984113	infinite	0.06450	0.00109	0.7048	0.0286	0.0795	0.0030	758	36	493	19	34.9
7	376325	infinite	0.06816	0.00089	0.7538	0.0277	0.0791	0.0028	873	27	491	18	43.8
8	1204977	95	0.05630	0.00092	0.5266	0.0327	0.0700	0.0042	464	36	436	26	6.1
9 core	399830	infinite	0.06306	0.00136	0.6876	0.0276	0.0782	0.0028	710	46	486	17	31.6
9 rim	521364	infinite	0.06086	0.00106	0.6663	0.0253	0.0790	0.0028	634	38	490	17	22.8
10	134260	infinite	0.07692	0.00181	0.8626	0.0371	0.0794	0.0030	1119	47	492	18	56.0
11	62421	infinite	0.05854	0.00095	0.6486	0.0235	0.0778	0.0026	550	35	483	16	12.2
12	272661	infinite	0.06041	0.00098	0.6621	0.0249	0.0786	0.0028	618	35	488	17	21.1
13	195166	20	0.04985	0.00354	0.4519	0.0389	0.0676	0.0034	188	165	422	21	−124.5
14	724837	infinite	0.07223	0.00163	0.8111	0.0315	0.0809	0.0027	992	46	502	17	49.4
15	244489	infinite	0.06778	0.00203	0.7360	0.0335	0.0777	0.0028	862	62	482	17	44.0
16	40380	infinite	0.05773	0.00094	0.6739	0.0277	0.0830	0.0032	520	36	514	20	1.1
17	401403	infinite	0.06445	0.00134	0.7117	0.0399	0.0801	0.0043	757	44	497	26	34.3
18	175680	infinite	0.05750	0.00063	0.6501	0.0213	0.0802	0.0026	511	24	497	16	2.6
19	403767	infinite	0.06395	0.00184	0.6840	0.0310	0.0778	0.0028	740	61	483	18	34.8
20	221787	infinite	0.06990	0.00129	0.7533	0.0271	0.0766	0.0025	926	38	476	15	48.6
21	**17226**	**infinite**	**0.05719**	**0.00207**	**0.6469**	**0.0327**	**0.0802**	**0.0029**	**499**	**80**	**497**	**18**	**0.4**
22	327093	infinite	0.06515	0.00087	0.7333	0.0281	0.0805	0.0030	779	28	499	19	36.0
23	255118	infinite	0.05734	0.00061	0.6224	0.0220	0.0777	0.0027	505	23	482	17	4.4
24	282525	infinite	0.06244	0.00080	0.6755	0.0256	0.0783	0.0029	689	27	486	18	29.5

Analysis #	Spot size um	^{206}Pb cps	^{206}Pb ^{238}U measured	2s error	^{207}Pb ^{206}Pb measured	2s error	%Rad. ^{206}Pb	^{206}Pb ^{238}U corrected	2s error	^{206}Pb ^{238}U Age (Ma)	2s error
NF-TUP–201–Nova Friburgo Granite–Titanite											
1	40	70208	0.0832	0.0028	0.1259	0.0021	92.7	0.0771	0.0026	479	16
2	40	130872	0.0834	0.0037	0.1240	0.0017	92.9	0.0775	0.0035	481	21
3	40	216502	0.0783	0.0026	0.0804	0.0012	97.5	0.0764	0.0026	474	16
4	40	92172	0.0818	0.0027	0.1027	0.0022	95.1	0.0778	0.0026	483	16
5	40	79857	0.0849	0.0028	0.1108	0.0012	94.3	0.0801	0.0027	497	17
6	40	84284	0.0945	0.0041	0.2184	0.0066	82.8	0.0783	0.0034	486	21
7	40	89139	0.0832	0.0029	0.1010	0.0025	95.3	0.0793	0.0028	492	17
8	40	134845	0.0897	0.0036	0.1663	0.0100	88.4	0.0793	0.0032	492	20
9	40	97337	0.0789	0.0025	0.0998	0.0013	95.4	0.0753	0.0024	468	15
10	40	93519	0.0795	0.0026	0.1073	0.0041	94.7	0.0752	0.0025	468	16
11	40	51250	0.0768	0.0025	0.1108	0.0013	94.3	0.0724	0.0024	451	15
12	40	91919	0.0787	0.0025	0.1004	0.0015	95.4	0.0751	0.0024	467	15
13	40	58621	0.0877	0.0029	0.1425	0.0049	90.9	0.0797	0.0026	495	16
14	40	62166	0.0845	0.0031	0.1153	0.0014	93.8	0.0793	0.0029	492	18
15	40	76623	0.0836	0.0029	0.1135	0.0019	94.0	0.0786	0.0027	488	17
16	40	65811	0.0877	0.0035	0.1253	0.0037	92.7	0.0813	0.0032	504	20
17	40	66163	0.0856	0.0032	0.1222	0.0014	93.1	0.0797	0.0029	494	18
18	40	63922	0.0849	0.0028	0.1235	0.0015	92.9	0.0789	0.0026	489	16
19	40	102457	0.0796	0.0028	0.1013	0.0049	95.3	0.0758	0.0027	471	17
20	40	77283	0.0840	0.0028	0.1186	0.0034	93.4	0.0785	0.0026	487	16
21	40	43202	0.1958	0.0098	0.6206	0.0112	40.1	0.0785	0.0039	487	24
22	40	127716	0.0855	0.0031	0.1188	0.0023	93.4	0.0798	0.0029	495	18
23	40	210777	0.0871	0.0054	0.1559	0.0312	89.5	0.0779	0.0048	484	30
24	40	64066	0.0885	0.0030	0.1392	0.0023	91.3	0.0807	0.0027	500	17
25	40	67748	0.0850	0.0030	0.1243	0.0016	92.8	0.0789	0.0027	489	17
26	40	143719	0.1041	0.0035	0.2900	0.0041	75.2	0.0783	0.0027	486	17

Grain #	^{206}Pb cps	^{206}Pb/^{204}Pb	^{207}Pb/^{206}Pb	2s error	^{207}Pb/^{235}U	2s error	^{206}Pb/^{238}U	2s error	^{207}Pb/^{206}Pb Age (Ma)	2s error	^{206}Pb/^{238}U Age (Ma)	2s error	discord. %
JA-FM–02–Sana Granite Zircon													
1	**460780**	**infinite**	**0.05695**	**0.00058**	**0.6398**	**0.0242**	**0.0805**	**0.0030**	**490**	**22**	**499**	**19**	**−1.9**
2	210311	infinite	0.05835	0.00072	0.6644	0.0233	0.0810	0.0028	543	27	502	17	7.5
3	129511	infinite	0.05824	0.00067	0.6382	0.0223	0.0776	0.0027	539	25	482	17	10.6
4	170162	infinite	0.05844	0.00075	0.6236	0.0246	0.0762	0.0029	546	28	473	18	13.4
5	619977	infinite	0.05922	0.00065	0.6931	0.0250	0.0844	0.0030	575	24	522	19	9.2
6	166635	infinite	0.05877	0.00074	0.6618	0.0256	0.0798	0.0030	559	27	495	19	11.4
7	78437	infinite	0.05759	0.00081	0.6241	0.0230	0.0778	0.0028	514	31	483	17	6.0
8	638060	infinite	0.05846	0.00066	0.5253	0.0319	0.0644	0.0039	547	25	402	24	26.4
9	185066	infinite	0.05774	0.00067	0.6521	0.0227	0.0799	0.0027	520	25	496	17	4.7
10	209068	infinite	0.05746	0.00067	0.6284	0.0298	0.0778	0.0037	509	26	483	23	5.2
11	146999	infinite	0.05850	0.00067	0.6584	0.0237	0.0802	0.0028	549	25	497	18	9.4
12	448791	infinite	0.12836	0.00201	5.1024	0.3759	0.2778	0.0202	2076	28	1580	115	23.9
13	635759	infinite	0.05797	0.00066	0.6453	0.0246	0.0800	0.0030	529	25	496	19	6.1
14	183877	infinite	0.05945	0.00071	0.6817	0.0239	0.0812	0.0028	584	26	503	17	13.8
15	205241	infinite	0.06226	0.00119	0.6758	0.0267	0.0775	0.0028	683	41	481	17	29.5
16	87924	infinite	0.05733	0.00061	0.6383	0.0249	0.0785	0.0031	504	24	487	19	3.4
17	**539386**	**26969**	**0.05689**	**0.00082**	**0.6162**	**0.0226**	**0.0776**	**0.0027**	**487**	**32**	**482**	**17**	**1.2**
18	112540	infinite	0.05872	0.00070	0.6713	0.0271	0.0802	0.0032	557	26	497	20	10.7
19	109504	infinite	0.05827	0.00078	0.6371	0.0255	0.0770	0.0030	540	29	478	19	11.5
20	55040	infinite	0.05762	0.00083	0.6362	0.0248	0.0784	0.0029	515	32	486	18	5.6
21	97838	infinite	0.06067	0.00071	0.7872	0.0333	0.0913	0.0038	627	25	564	24	10.2
22	61935	infinite	0.05892	0.00098	0.6601	0.0260	0.0796	0.0029	564	36	494	18	12.5
23	1016460	4983	0.10740	0.00120	3.4217	0.1644	0.2296	0.0110	1756	20	1332	64	24.1
24	63430	infinite	0.05966	0.00096	0.6749	0.0257	0.0788	0.0028	591	35	489	18	17.3

References

Almeida, R.P., Janikian, L., Fragoso César, A.R.S., Fambrini, G.L., 2008. The Ediacaran to Cambrian rift system of southeastern South America: tectonic implications. Journal of Geology 118, 145–161.

De Campos, C.P., Mendes, J.C., Ludka, I.P., Medeiros, S.R., Moura, J.C., Wallfass, C., 2004. A review of the Brasiliano magmatism in southern Espírito Santo, Brazil, with emphasis on post-collisional magmatism. ISSN 1441-8142. Journal of the Virtual Explorer, Electronic Edition vol. 17, 35. Paper 1.

Heilbron, M., Machado, N., 2003. Timing of terrane accretion in the Neoproterozoic–Eopaleozoic Ribeira orogen (SE Brazil). Precambrian Research 125, 87–112.

Heilbron, M., Schmitt, R., Mohriak, W., Trouw, R.A.J., 2003. Geology of The Cabo Frio Region, Rio de Janeiro State, Brazil. In: Chaves, H., et al. (Eds.), Field Trips of the 31st International Geological Congress, 2000 (CD-ROM). Rio de Janeiro.

Heilbron, M., Valeriano, C.M., Tassinari, C.C.G., Almeida, J.C.H., Tupinambá, M., Siga Junior, O., Trouw, R.A.J., 2008. Correlation of Neoproterozoic terranes between Ribeira Belt, SE Brazil and its African counterpart: comparative tectonic evolution and open questions. In: Pankhurst, R.J., Trouw, R.A.J., de Brito Neves, B.B., de Wit, M.J. (Eds.), West Gondwana: Pre-Cenozoic Correlations Across the South Atlantic Region, 294. Geological Society, London, pp. 211–237. Special Publications.

Janasi, V.A., Leite, R.J., van Schmus, W.R., 2001. U-Pb chronostratigraphy of the granitic magmatism in the Agudos Grandes batholith (west of São Paulo, Brazil) - implications for the evolution of the Ribeira belt. Journal of South American Earth Sciences 14, 363–376.

Junho, M.C.B., Weber-Diefenbach, K.C.M., Penha, H.M., 1987. Major and minor elements geochemistry of the Pedra Branca, Frades and Nova Friburgo granitic complexes, Ribeira mobile belt, Brasil. Revista Brasileira de Geociências 17, 507–511.

Ledru, P., Courrioux, G., Dallain, C., Lardeaux, J.M., Montel, J.M., Vanderhaeghe, O., Vitel, G., 2001. The Velay dome (French Massif Central): melt generation and granite emplacement during orogenic evolution. Tectonophysics 342, 207–237.

Leite, R.J., Heaman, L.H., Janasi, V.A., Martins, L., Creaser, R.A., 1997. The late- to post-orogenic transition in the Neoproterozoic Agudos Grandes granite batholith (Apiaí domain, SE Brazil): constraints from geology, mineralogy, and U-Pb geochronology. Journal of South American Earth Sciences 23, 193–212.

Ludwig, K.R., 2003. User's manual for Isoplot 3.00: a geochronological toolkit for Microsoft Excel. Berkeley Geochronology Center Special Publication 4, 70.

Machado, N., Valladares, C.S., Heilbron, M., Valeriano, C.M., 1996. U-Pb geochronology of Central Ribeira belt. Precambrian Research 79, 347–361.

Mendes, J.C., Ávila, C., Mello, Ronaldo, Heilbron, M., Moura, C., 2006. $^{207}Pb/^{206}Pb$-ages of zircons from syn-collisional I-type porphyritic granites of the central Ribeira belt, SE Brazil. Gondwana Research 9, 326–336.

Pires, F.R.M., Valença, J., Ribeiro, A., 1982. Multistage generation of granite in Rio de Janeiro, Brazil. Anais da Academia Brasileira de Ciências 54, 563–574.

Pedrosa-Soares, A.C., Noce, C.M., Wiedemann, C., Pinto, C.P., 2001. The Araçuaí-West-Congo orogen in Brazil, an overview of a confined orogen formed during Gondwanaland assembly. Precambrian Research 110, 307–323.

Pedrosa-Soares, A.C., Alkmim, F.F., Tack, L., Noce, C.M., Babinski, M., Silva, L.C., Martins-Neto, M.A., 2008. Similarities and Differences Between the Brazilian and African Counterparts of the Neoproterozoic Araçuaí-West Congo Orogen, 294. Geological Society, London. Special Publications153–172.

Porto Jr., R., Figueiredo, M.C.H., 1996. Petrology of the Granites from Pedra Branca Range, Rio de Janeiro, RJ, Brazil, vol. 18. Boletim IG-USP. Série Científica, São Paulo. Publicação Especial43–47.

Rey, P., Vanderhaeghe, O., Teyssier, C., 2001. Gravitational collapse of the continental crust, definition, regimes and modes. Tectonophysics 342, 435–449.

Schmitt, R.S., Trouw, R.A.J., Van Schmus, W.R., Pimentel, M.M., 2004. Late amalgamation in the central part of Western Gondwana, new geochronologicalal data and the characterization of a Cambrian collision orogeny in the Ribeira belt (SE Brazil). Precambrian Research 133, 29–61.

Silva, L.C., McNaughton, N.J., Hartmann, L.A., Fletcher, I.R., 2003. Zircon U-Pb SHRIMP dating of the Serra dos Órgãos and Rio de Janeiro gneissic granitic suítes, implications for the (560 Ma) Brasiliano/Panafrican collage. Revista Brasileira de Geociências 33, 237–244.

Simonetti, A., Heaman, L.M., Hartlaub, R.P., Creaser, R.A., McHattie, T.G., Bohm, C.O., 2005. U-Pb zircon dating by laser ablation-MC-ICP-MS using a new multiple ion counting-faraday collector array. Journal of Analytical Atomic Spectrometry 20, 677–686.

Simonetti, A., Heaman, L.M., Chacko, T., Banerjee, N.R., 2006. In situ petrographic thin section U-Pb dating of zircon, monazite, and titanite using laser ablation-MC-ICP-MS. International Journal of Mass Spectrometry 253, 87–97.

Simonetti, A., Heaman, L.M., Chacko, T., 2008. Use of discrete-dynode secondary electron multipliers with faradays – a 'reduced volume' approach for in situ U-Pb dating of accessory minerals within petrographic thin sections by LA-MC-ICPMS. In: Sylvester, P. (Ed.), Laser Ablation-ICP-MS in the Earth Sciences Current Practices and Outstanding Issues. Short Course Series, 40. Mineralogical Association of Canada, pp. 241–264.

Söllner, F., Lammerer, B., Weber-Diefenbach, K., Hansen, B.T., 1987. The Brasiliano orogenesis, age determinations (Rb-Sr and U-Pb) in the coastal mountain region of Espírito Santo, Brazil. Zentralblatt für Geologie und Paläontologie, Teil I 7/8, 729–741.

Söllner, F., Lammerer, B., Wiedemann-Leonardos, C., 2000. Dating the Ribeira mobile belt. In: Miller, H., Hervé, F. (Eds.), Geoscientific Cooperation with Latin America. 31st International Geological Congress, Rio de Janeiro 2000, 1. Zeitschrift für Angewandte Geologie, pp. 245–255. Sonderheft SH.

Tera, F., Wasserburg, G.J., 1972. U-Th-Pb systematics in three Apollo 14 basalts and the problem of initial Pb in lunar rocks. Earth and Planetary Science Letters 14, 281–304.

Tupinambá, M., Teixeira, W., Heilbron, M., 2000. Neoproterozoic Western Gondwana assembly and subduction-related plutonism, the role of the Rio Negro complex in the Ribeira belt, south-eastern Brazil. Revista Brasileira de Geociências 30, 7–11.

Tupinambá et al., (in press). Explanatory Note to the Geologic Map of the Nova Friburgo sheet (1,100.000 scale). CPRM Brazilian Geologic Survey, Geobank (http://geobank.sa.cprm.gov.br/).

Unrug, R., 1996. The assembly of Gondwanaland. Episodes 19, 11–20.

Valeriano et al., (in press). Explanatory Note to the Geologic Map of the Baía de Guanabara sheet (1,100.000 scale). CPRM - Brazilian Geologic Survey, Geobank (http://geobank.sa.cprm.gov.br/).

Vanderhaeghe, O., Teyssier, C., 2001. Partial melting and flow of orogens. Tectonophysics 342 (2001), 451–472.